Sustainable Chemical Engineering
https://ojs.wiserpub.com/index.php/SCE/

UNIVERSAL WISER PUBLISHER

Research Article

# Sustainable Removal of Methyl Violet from Aqueous Solution Using Banana Peel Extract-Modified Magnetite Adsorbent

**Addina Husna Fillah, Maya Rahmayanti***

Chemistry Study Program, Sunan Kalijaga State Islamic University Yogyakarta, Papringan, Caturtunggal, Depok, Sleman, Yogyakarta, 55281, Indonesia
E-mail: maya.rahmayanti@uin-suka.ac.id

**Received:** 21 August 2025; **Revised:** 26 September 2025; **Accepted:** 9 October 2025

**Abstract:** The textile industry generates large volumes of dye-containing effluents, with Methyl Violet (MV) among the most toxic and persistent pollutants due to its carcinogenicity and resistance to degradation. In this study, a green adsorbent based on magnetite ($Fe_3O_4$) modified with Banana Peel (BP) extract was synthesized via reverse co-precipitation, where BP functions simultaneously as a natural reducing, stabilizing, and surface-functionalizing agent. Structural characterization using X-Ray Diffraction (XRD) and Fourier-Transform Infrared (FTIR) spectroscopy confirmed the crystalline spinel structure of $Fe_3O_4$ and the incorporation of organic functional groups (-OH, C=O) from BP onto its surface. Adsorption experiments demonstrated a maximum capacity of 135 $mg \cdot g^{-1}$ for MV at pH 6.0, with data fitting well to the Langmuir isotherm model, indicating monolayer adsorption. Furthermore, $Fe_3O_4$-BP achieved over 95% MV removal in simulated wastewater and could be magnetically separated and reused. These findings emphasize the dual role of agricultural waste as both a sustainable reagent in nanoparticle synthesis and as a performance enhancer for adsorption, underscoring the potential of $Fe_3O_4$-BP as a cost-effective and eco-friendly material for wastewater treatment.

***Keywords*:** banana peel extract, magnetite, methyl violet, adsorption, sustainable materials

## 1. Introduction

The textile industry is one of the major sectors of the global economy, but it also represents a primary source of water pollution through wastewater containing synthetic dyes.[1] Dyes such as methyl violet are toxic, carcinogenic, and resistant to natural degradation, posing serious threats to aquatic ecosystems and human health.[2] Various wastewater treatment methods have been developed, including coagulation, photocatalysis, and advanced oxidation processes. These methods have been widely applied due to their established performance; however, they suffer from several critical drawbacks, including high operational costs, generation of secondary sludge, poor selectivity, and limited reusability of the materials involved. For example, coagulation and oxidation processes often require large amounts of chemical reagents and produce hazardous by-products, while activated carbon although highly effective, remains costly and difficult to regenerate. Similarly, membrane processes are energy-intensive and prone to fouling, restricting their large-scale use in developing regions. Among these techniques, adsorption is a simple, efficient, and relatively low-cost method with strong potential for sustainable applications.[3-5]


DOI: https://doi.org/10.37256/sce.7120268345

Developing adsorbent materials from biomass has become a key priority in implementing the principles of green chemistry. Agricultural wastes such as date seeds, coconut shells, and fish scales have been demonstrated to be effective precursors for synthesizing eco-friendly adsorbents capable of removing dyes from wastewater.[6-8] Among these biomass sources, banana peels are beneficial due to their high polyphenol content and abundant functional groups, which not only enhance surface stability but also serve as natural reducing agents in the synthesis of metal oxides, thereby enabling the green and efficient formation of magnetite.[9-11]

Magnetite is one of the most extensively studied materials owing to its high adsorption capacity for dyes and its magnetic properties, which facilitate easy separation after use. Nevertheless, $Fe_3O_4$ nanoparticles often suffer from agglomeration and limited surface functionality, which can reduce their adsorption efficiency in practical applications. In addition, the use of hazardous synthetic stabilizers in conventional synthesis routes raises environmental concerns. Magnetic materials, have been shown to improve adsorption capacity for cationic dyes such as methyl violet and crystal violet.[12,13] Green synthesis approaches are also regarded as crucial for producing materials that are not only effective but also environmentally sustainable.[14] However, studies employing banana peel extract as a natural reducing and stabilizing agent in magnetite synthesis remain scarce, indicating a significant research gap. In addition, Banana Peel (BP) provides abundant polyphenols and organic functional groups that become incorporated onto the $Fe_3O_4$ surface, thereby enriching the number of active sites available for adsorption. This surface modification is expected to enhance the interaction between $Fe_3O_4$-BP and cationic dye molecules, leading to improved methyl violet adsorption performance.

This study aims to develop banana peel extract–based magnetite ($Fe_3O_4$-BP) through a green synthesis route as an effective adsorbent for removing methyl violet from aqueous solutions. The synthesis was carried out via a reverse co-precipitation method, in which banana peel extract functioned as a natural reducing agent and surface stabilizer. Fourier-Transform Infrared (FTIR) spectroscopy and X-Ray Diffraction (XRD) were used to characterize the formation of crystalline magnetite structures with additional functional groups derived from the biomass. These findings highlight the potential of banana peel waste as a sustainable source of functional materials, offering a low-cost and environmentally friendly solution for textile wastewater treatment.

# 2. Materials and methods

## 2.1 *Materials*

Banana peels were collected from local household waste in research location. Ferric chloride hexahydrate ($FeCl_3 \cdot 6H_2O$, ≥ 98%, Merck), ferrous sulfate heptahydrate ($FeSO_4 \cdot 7H_2O$, ≥ 99%, Merck), and sodium hydroxide (NaOH, Merck) were used as precursors. Methyl violet ($C_{24}H_{28}ClN_3$, Sigma-Aldrich) served as the model dye pollutant. All chemicals were of analytical grade and used without further purification. Distilled water was employed in all preparations and experimental procedures.

## 2.2 *Methods*

### 2.2.1 *Preparation of banana peel extract*

Fresh banana peels were washed with tap water, air-dried at room temperature for 48 h, and cut into small pieces. About 50 g of peels was boiled in 500 mL of distilled water for 30 min, and the mixture was filtered through Whatman No. 42 filter paper to obtain the extract (final yield ≈ 450-470 mL). Although other separation methods such as centrifugation or vacuum filtration could be applied, gravity filtration was considered sufficient for obtaining a clear extract, which was then stored at 4 °C until use.

### 2.2.2 *Green synthesis of banana peel-assisted magnetite ($Fe_3O_4$-BP)*

$Fe_3O_4$-BP was synthesized via the coprecipitation method following the stoichiometric requirement of $Fe_3O_4$. An aqueous solution of $FeCl_3 \cdot 6H_2O$ (0.1 M) and $FeSO_4 \cdot 7H_2O$ (0.05 M) was prepared with a $Fe^{3+}/Fe^{2+}$ molar ratio of 2 : 1, which corresponds to the spinel structure of magnetite (two $Fe^{3+}$ and one $Fe^{2+}$ per formula unit). Fifteen milliliters of banana peel extract was then gradually added as a natural reducing and stabilizing agent under continuous stirring at 80 °C. Subsequently, a 1 M NaOH solution was added dropwise until pH ≈ 11, leading to the coprecipitation reaction:

$$Fe^{2+} + 2Fe^{3+} + 8OH^- \rightarrow Fe_3O_4\,(S) + 4H_2O \quad (1)$$

This process yielded a black magnetite precipitate, which was collected using an external magnet, repeatedly washed with distilled water until a neutral pH, and dried at 60 °C for 12 h.

#### 2.2.3 *Characterization*

Fourier-Transform Infrared spectroscopy (FTIR, Shimadzu IRPrestige-21) was used to identify surface functional groups. X-Ray Diffraction (XRD, PANalytical X'Pert PRO) was employed to examine the crystallinity and estimate crystallite size using the Debye-Scherrer equation. Scanning Electron Microscopy (SEM, JEOL JSM-6510LA) was conducted to observe surface morphology.

#### 2.2.4 *Batch adsorption experiments*

Batch adsorption studies were conducted at different pH values (3-9) to determine the optimum conditions. In each experiment, 50 mL of methyl violet solution (10-50 mg/L) was mixed with 0.05 g of $Fe_3O_4$-BP in a 100 mL Erlenmeyer flask and shaken at 150 rpm for 60 min. After equilibrium, the adsorbent was magnetically separated, and the residual dye concentration was quantified using a Ultraviolet-Visible (UV-Vis) spectrophotometer (Shimadzu UV-1800) at 584 nm.

#### 2.2.5 *Adsorption isotherm studies*

The adsorption data were analyzed using the Langmuir and Freundlich isotherm models to determine the maximum adsorption capacity ($q_{max}$) and the interaction mechanism between methyl violet and $Fe_3O_4$-BP. The linear equation of the Langmuir model is presented in Equation (2):

$$\frac{C_e}{q_e} = \frac{1}{q_{max} K_L} + \frac{C_e}{q_{max}} \quad (2)$$

where $C_e$ (mg/L) is the equilibrium concentration, $q_e$ (mg/g) is the amount of dye adsorbed at equilibrium, $q_{max}$ (mg/g) is the maximum adsorption capacity, and $K_L$ (L/mg) is the Langmuir constant.

The Freundlich model is presented in Equation (3):

$$\ln q_e = \ln K_F + \frac{1}{n} \ln C_e \quad (3)$$

where $K_F$ (L/mg) is the Freundlich constant related to the adsorption capacity, and $1/n$ represents the adsorption intensity.

## 3. Result and discussion

### 3.1 *Characterization of banana peel-assisted magnetite ($Fe_3O_4$-BP)*

FTIR analysis (Figure 1) revealed that pure $Fe_3O_4$ exhibited only the characteristic Fe-O band at 578 $cm^{-1}$, whereas the BP extract displayed major functional groups at 3,332 $cm^{-1}$ (O-H), 2,939 $cm^{-1}$ (C-H), 1,589 $cm^{-1}$ (aromatic C=C), 1,396 $cm^{-1}$ (C-O), and 1,064 $cm^{-1}$ (C-O-C), indicating the presence of phenolic compounds, flavonoids, and organic acids.[15-17] In $Fe_3O_4$-BP, the Fe-O peak shifted to 570 $cm^{-1}$, suggesting surface modification due to interactions between $Fe^{2+}$/$Fe^{3+}$ ions in the $Fe_3O_4$ lattice and the functional groups from BP, which induced local distortion and changes in bond strength. Peaks at 3,425 $cm^{-1}$ (O-H), 1,620 $cm^{-1}$ (C=O), 1,342 $cm^{-1}$ (C-O), and 1,095 $cm^{-1}$ (C-O-C) remained observable with variations in position and intensity, particularly the shift of C=O from ~ 1,700 $cm^{-1}$ to 1,620 $cm^{-1}$ and

the emergence of a C-O peak at 1,342 $cm^{-1}$, characteristic of coordinated carboxylates.[18,19] These changes indicate that the organic groups from BP were not only physically adsorbed but also formed coordination bonds, possibly in bidentate or monodentate modes, with the $Fe_3O_4$ surface, yielding Fe-OOC-R complexes.[20] Such interactions demonstrate the dual role of banana peel extract as both a reducing and binding agent,[21] underpinning the green synthesis of iron-based magnetic materials in the absence of synthetic surfactants.

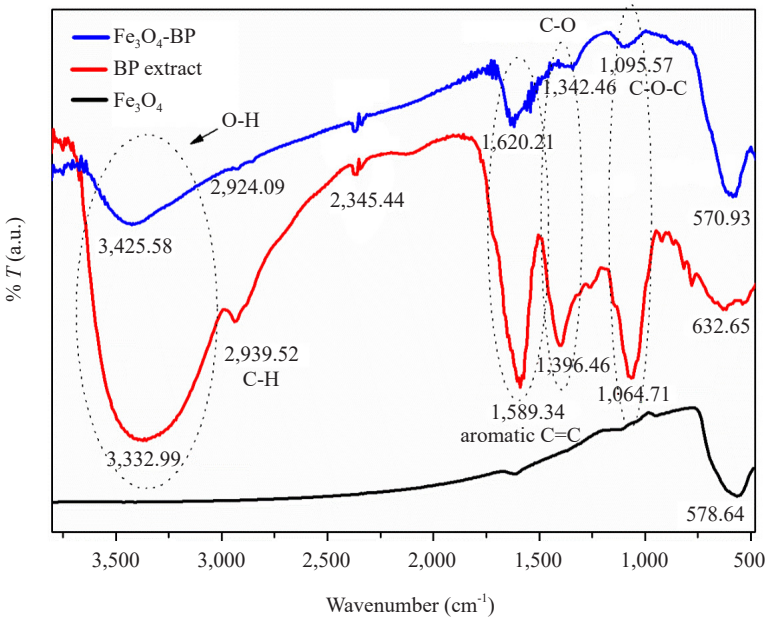


**Figure 1.** FTIR spectra of $Fe_3O_4$, BP extract, and $Fe_3O_4$-BP, showing characteristic absorption bands for functional groups and confirming the successful surface modification of $Fe_3O_4$ by banana peel extract

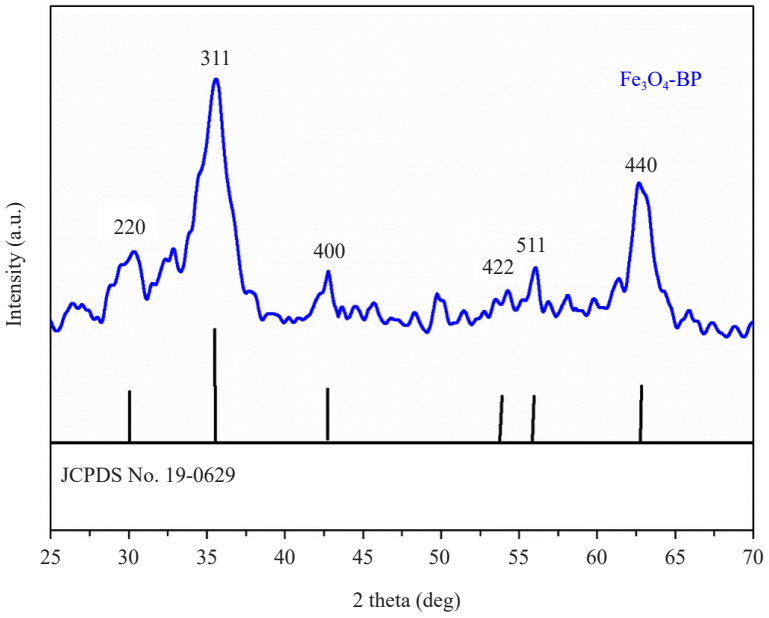


**Figure 2.** XRD pattern of $Fe_3O_4$-BP, showing diffraction peaks indexed to the spinel structure of magnetite ($Fe_3O_4$) with reference to JCPDS No. 19-0629, confirming the crystalline phase of the synthesized material

These findings are consistent with previous studies that report that plant extracts, particularly those rich in phenolics and carboxylic acids, can chemically interact with iron oxide surfaces through the formation of coordination bonds, thereby contributing not only to metal ion reduction but also to the stabilization of green-synthesized materials. The present results reinforce the notion that banana peel extract is an effective and reliable biogenic agent for $Fe_3O_4$ functionalization, in line with the growing trend of developing sustainable, nature-derived materials.

The XRD spectrum of $Fe_3O_4$-BP (Figure 2) exhibited major diffraction peaks at $2\theta \approx 30.1°$, 35.5°, 43.1°, 53.4°, 57.0°, and 62.8°, which correspond to the crystallographic planes (220), (311), (400), (422), (511), and (440) of the cubic spinel structure of magnetite ($Fe_3O_4$) (JCPDS No. 19-0629). The most intense peak at 35.5° (311) is a key characteristic of magnetite. The absence of additional peaks corresponding to secondary phases such as $\alpha$-$Fe_2O_3$ or $\gamma$-$Fe_2O_3$ confirm the successful formation of a pure $Fe_3O_4$ phase.

The relatively broad reflections, particularly at (311), suggest the presence of small crystallites. The average crystallite size was estimated to be 3.62 nm using the Debye-Scherrer equation, which confirms the nanocrystalline nature of the material. This method provides crucial information about the size of the crystal domains, a key parameter directly related to adsorption capacity, as smaller crystallites generally have higher surface energy and more active sites.

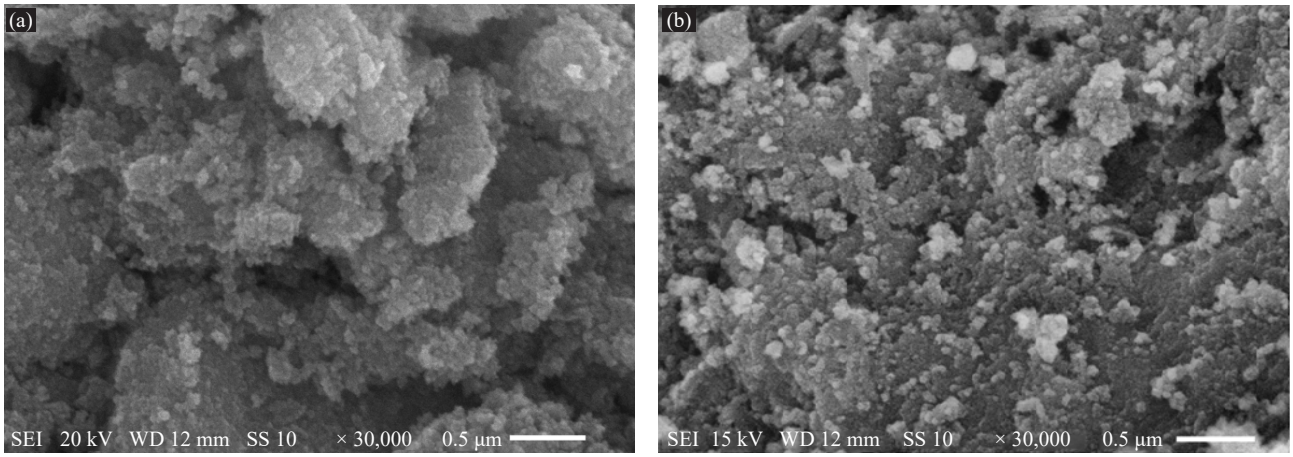


**Figure 3.** Scanning Electron Microscope (SEM) images of $Fe_3O_4$ (a) and $Fe_3O_4$-BP (b)

Furthermore, several recent studies on $Fe_3O_4$ modified with plant extracts have also reported irregular and agglomerated morphologies.[22,23] The SEM images in this study further support these findings (Figure 3). In the SEM image of $Fe_3O_4$ (Figure 3a), dense aggregates composed of primary nanometer-sized grains closely attached to each other can be observed. Based on the scale bar of 0.5 µm (500 nm) at a magnification of × 30,000, the diameter of the primary grains is estimated to be in the range of ~ 50-200 nm, while the formed aggregates are larger, reaching several hundred nanometers. This morphology, which indicates strong agglomeration, is consistent with the interparticle binding phenomenon commonly found in unmodified magnetic nanoparticles. In the SEM image of $Fe_3O_4$-BP (Figure 3b), the grains appear finer, and the surface shows a more porous structure with a smaller and more heterogeneous particle size distribution compared to pure $Fe_3O_4$. A visual comparison with the scale bar suggests that the primary grains in $Fe_3O_4$-BP are likely in the range of ~ 20-100 nm, with many grains appearing around one-tenth to one-fifth of the scale bar length (50-100 nm), and some even smaller, approaching 20-30 nm. The reduction in primary particle size and the lower degree of agglomeration indicate that the addition of BP modifies the growth and aggregation process of $Fe_3O_4$, thereby enhancing the effective surface area.

Based on a comparison with previous reports, the use of banana peel extract has been shown to produce smaller crystallites, as presented in Table 1. This confirms its role as an effective stabilizing agent in reducing agglomeration and suppressing excessive crystal growth during synthesis.

**Table 1.** Comparative analysis of $Fe_3O_4$ synthesis using plant extracts: Precursor systems, synthesis conditions, Scherrer-estimated crystallite size, morphology, particle size and reference sources (2019-2024)

| $Fe_3O_4$/Plant extracts | Precursor | Synthesis method | Crystallite size (nm) | Morphology/Particle size (nm) | Ref. |
|---|---|---|---|---|---|
| $Fe_3O_4$/*Archidendron pauciflorum* extract (15 mL) | $FeSO_4 \cdot 7H_2O$ and $FeCl_3 \cdot 6H_2O$, NaOH | Reverse Co-precipitation, 60 °C, 60 min | 15 | -/318.3 nm | 24 |
| $Fe_3O_4$/*Parkia speciossa* extract (15 mL) | $FeSO_4 \cdot 7H_2O$ and $FeCl_3 \cdot 6H_2O$, NaOH | Reverse Co-precipitation, 60 °C, 60 min | 11.3 | -/5.4, 195, and 2,702.6 nm | 25 |
| Pure $Fe_3O_4$ | $FeSO_4 \cdot 7H_2O$ and $FeCl_3 \cdot 6H_2O$, $NH_4OH$ | Co-precipitation, 60 °C, 30 min | 19.9 | Spherical shapes/20.7 nm | 26 |
| $Fe_3O_4$/*Moringa oleifera* extract | $FeSO_4 \cdot 7H_2O$ and $FeCl_3 \cdot 6H_2O$, $NH_4OH$ | Co-precipitation, 60 °C, 30 min | 15.7-16.1 | Spherical shapes/21.1 nm | 26 |
| $Fe_3O_4$/*Archidendron pauciflorum* extract (15 mL) | $FeSO_4 \cdot 7H_2O$ and $FeCl_3 \cdot 6H_2O$, NaOH | Sonochemical, Reverse Co-precipitation, room temperature, 60 min | 17.0 | Rough surface/2.56 nm, 862.23 nm, and 4,855.78 nm | 27 |
| $Fe_3O_4$/Tea dregs extract (15 mL) | $FeSO_4 \cdot 7H_2O$ and $FeCl_3 \cdot 6H_2O$, NaOH | Reverse Co-precipitation, room temperature, 60 min | 18.9 | -/2,670 nm | 28 |
| Pure $Fe_3O_4$ | $FeSO_4 \cdot 7H_2O$ and $FeCl_3 \cdot 6H_2O$, NaOH | Reverse Co-precipitation, room temperature, 60 min | 15 | Rough surface/- | 29 |
| $Fe_3O_4$/Banana peel extract (15 mL) | $FeSO_4 \cdot 7H_2O$ and $FeCl_3 \cdot 6H_2O$, NaOH | Reverse Co-precipitation, 60 °C, 60 min | 3.62 | Irregular morphology with rough and porous surface structure/20-100 nm | This research |

## 3.2 *Effect of pH on methyl violet adsorption*

The adsorption efficiency of Methyl Violet (MV) onto $Fe_3O_4$-BP was strongly influenced by the solution pH, as shown in Figure 4. At low pH values (2-4), the adsorption percentage ranged between 78% and 84%, and then sharply increased to 89% at pH 6, remaining stable up to pH 10. These results indicate that pH 6 is the optimum condition for MV adsorption using $Fe_3O_4$-BP.

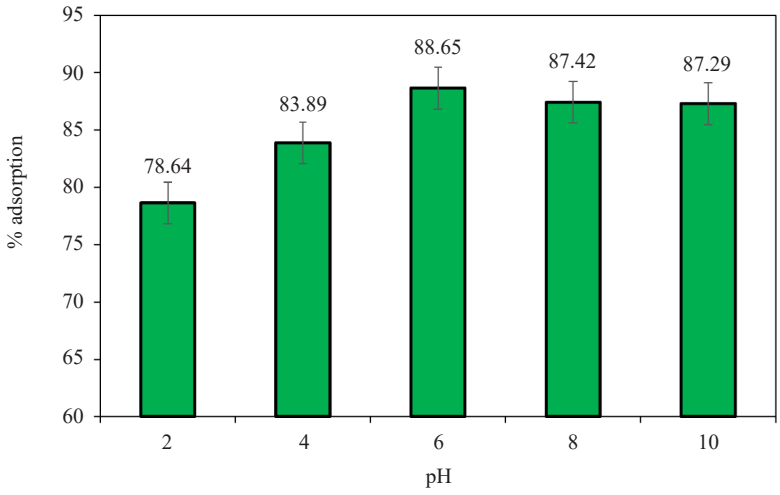


**Figure 4.** Effect of pH on the percentage adsorption of adsorbate by $Fe_3O_4$-BP

This behavior can be explained by changes in the surface charge of the adsorbent, which has a point of zero

charge ($pH_{PZC}$) around 6.4-7.5.[30,31] At pH < 6, the $Fe_3O_4$-BP surface becomes positively charged due to the protonation of hydroxyl groups ($-OH_2^+$), leading to electrostatic repulsion against the cationic MV molecules and thus hindering adsorption. At pH 6, the near-neutral surface minimizes repulsion, enabling non-electrostatic interactions such as $\pi$-$\pi$ stacking between the aromatic rings of MV and the carbonaceous structures of BP, as well as hydrogen bonding involving nitrogen and oxygen functional groups on the adsorbent surface. At pH > 6, the surface acquires a negative charge ($-O^-$), which can attract MV cations electrostatically. However, the adsorption efficiency does not further increase, as the adsorption capacity reaches its maximum, accompanied by competition from $OH^-$ ions occupying active sites.

## 3.3 *Adsorption isotherm studies*

Based on Figure 5, the adsorption percentage of MV dye onto $Fe_3O_4$-BP increased with the rise in initial concentration, reaching an optimum at 30 ppm. At lower concentrations (5-15 ppm), the adsorption efficiency remained relatively low (72-87%) because the limited number of MV molecules resulted in the underutilization of many active sites on the adsorbent surface.

As the concentration increased to 30 ppm, more MV molecules interacted with the adsorbent surface, leading to a higher adsorption efficiency, with a maximum value of 95.45%. At this point, an ideal balance was achieved between the available active sites of $Fe_3O_4$-BP and the MV molecules in solution. However, at higher concentrations (50 ppm), the adsorption efficiency decreased to 87% due to the limited number of active sites on the adsorbent surface. The excess MV molecules could not be adsorbed and remained in the solution, reducing the overall adsorption percentage.

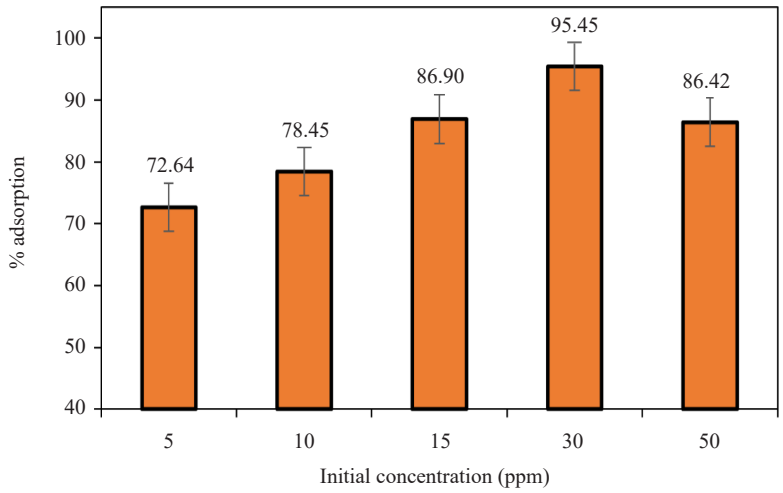


**Figure 5.** Percentage adsorption of methyl violet onto $Fe_3O_4$-BP at various initial concentrations (5-50 ppm) at 60 °C and 60 min

The adsorption isotherm analysis in Figure 6 revealed that the Langmuir model provided a better fit compared to the Freundlich model, with an $R^2$ value of 0.9936, which was significantly higher than of 0.6768. From the linear equation, the maximum adsorption capacity ($q_{max}$) was calculated to be 90.09 $mg \cdot g^{-1}$ with a Langmuir constant ($K_L$) of 1.50 $L \cdot mg^{-1}$, while the separation factor ($R_L$) ranged between 0.118 and 0.013, indicating that the adsorption process was highly favorable.

In contrast, the Freundlich parameters showed a $K_F$ value of 6.09 and an adsorption intensity ($n$) of 10.48, which also suggested favorable adsorption, although the overall model fit was poorer. Therefore, it can be concluded that the adsorption mechanism of methyl violet on $Fe_3O_4$-BP is better described by the Langmuir model, representing monolayer adsorption on a relatively homogeneous surface.

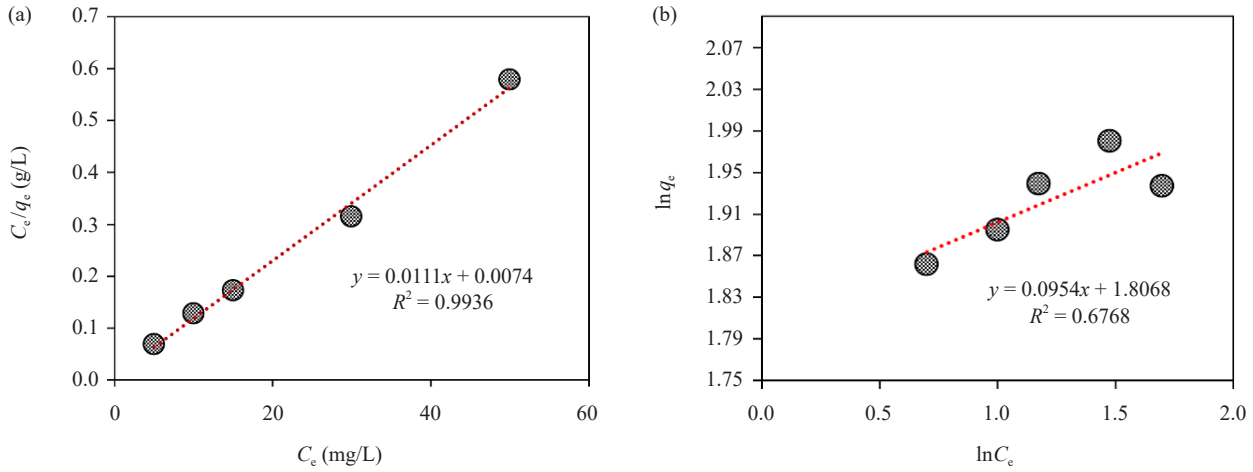


**Figure 6.** Langmuir adsorption isotherm model (a) and Freundlich adsorption isotherm model (b) (10 mg MNPs-BP, pH 6, 60 min)

## 3.4 *Comparative methyl violet adsorption performance with reported adsorbents*

The comparative adsorption performance of various reported adsorbents toward methyl violet is summarized in Table 2. Natural adsorbents such as Iraqi date seeds display a very low uptake capacity ($q_{max}$ = 0.98 mg/g), indicating the limitations of unmodified biomass materials. Simple composites such as coir-pith/$Fe_3O_4$ and HNT-$Fe_3O_4$ show a slight improvement in adsorption performance ($q_{max}$ = 3.14-20.04 mg/g), yet the values remain far below the requirements for practical industrial applications. On the other hand, highly engineered adsorbents such as Sodium Dodecyl Sulfate (SDS)-coated $Fe_3O_4$ exhibit remarkably high adsorption capacity ($q_{max}$ = 416.7 mg/g), although their application is constrained by the necessity of extremely acidic conditions. In contrast, the $Fe_3O_4$-BP developed in this study achieved a high adsorption capacity ($q_{max}$ = 135 mg/g), striking a balance between efficiency and operational feasibility.

**Table 2.** Comparison of adsorption isotherm models for methyl violet dye on various adsorbents

| Adsorbent | Adsorbate | Adsorption conditions | Isotherm model (Parameters) | Reference |
|---|---|---|---|---|
| Magnetic Nanoparticles-Black Phosphorus (MNPs-PT) (10 mg) | Methyl violet (15 ppm, 25 mL) | Room temperatur, pH 4, 60 min, 150 rpm | Freundlich ($R^2$ = 0.83, $n$ = 0.33, $K_F$ = 3.02 L/mg) | 2 |
| $KAlPO_4F$ (10 mg) | Methyl violet (15 ppm, 10 mL) | Room temperatur, pH 7, 10 min, 3,000 rpm | Freundlich ($R^2$ = 0.99, $n$ = 1.87, $K_F$ = 3.84 L/mg) | 3 |
| Iraqi date seeds (5 g) | Methyl violet (20 ppm, 50 mL) | Room temperatur, pH 6.5, 120 min | Langmuir ($R^2$ = 0.99, $q_{max}$ = 0.98 mg/g) | 32 |
| SDS-coated $Fe_3O_4$ (10 mg) | Methyl violet (5 ppm, 25 mL) | Room temperatur, pH 3, 10 min | Langmuir ($R^2$ = 0.99, $q_{max}$ = 416.7 mg/g, $K_L$ = 0.27 L/mg) | 33 |
| A halloysite-magnetite-based composite (HNT-$Fe_3O_4$) (10 mg) | Methyl violet (90 ppm, 25 mL) | Room temperatur, pH 4.2, 6 h | Langmuir ($R^2$ = 0.99, $q_{max}$ = 20.04 mg/g, $K_L$ = 0.11 L/mg) | 34 |
| Coir-pith/$Fe_3O_4$ (modified) | Methyl violet (90 ppm, 25 mL) | Room temperatur, pH 4.2, 6 h | Langmuir ($R^2$ = 0.99, $q_{max}$ = 3.14 mg/g, $K_L$ = 0.91 L/mg) | 35 |
| ZnO/$Fe_3O_4$ (1 g/L) | Methyl violet (50 ppm, 50 mL) | Room temperatur, pH 7, 12 h, 200 rpm | Freundlich ($R^2$ = 0.99, $n$ = 0.38, $K_F$ = 25.58 L/mg) | 36 |
| $Fe_3O_4$-BP (10 mg) (This research) | Methyl violet (50 ppm, 25 mL) | Room temperatur, pH 6, 60 min, 150 rpm | Langmuir ($R^2$ = 0.99, $q_{max}$ = 135 mg/g, $K_L$ = 1.50 L/mg) | This work |

In terms of adsorption isotherm modeling, several previously reported adsorbents, including MNPs-PT, $KAlPO_4F$, and $ZnO/Fe_3O_4$, were best fit with the Freundlich model, suggesting heterogeneous surface interactions. Meanwhile, $Fe_3O_4$-BP demonstrated excellent compliance with the Langmuir model ($R^2 = 0.99$), confirming a monolayer adsorption mechanism with more predictable and controllable adsorption behavior.

The comparison of operational conditions further highlights the advantages of $Fe_3O_4$-BP. Iraqi date seeds required prolonged contact time (120 min), while SDS-coated $Fe_3O_4$ was effective only under strongly acidic conditions (pH 3). $ZnO/Fe_3O_4$ also demanded high adsorbent dosage (1 g/L) and extended stirring (200 rpm, 120 min). By contrast, $Fe_3O_4$-BP reached optimal performance at near-neutral pH (6.0), low adsorbent dosage (10 mg), and a relatively short equilibrium time (60 min), indicating higher efficiency and easier applicability in real wastewater treatment scenarios.

From the sustainability perspective, raw biomass adsorbents are generally eco-friendly but suffer from insufficient adsorption performance, whereas synthetic nanocomposites with very high adsorption capacity typically involve energy-intensive processes or hazardous chemical modifications. $Fe_3O_4$-BP, however, combines bio-derived precursors with a relatively simple preparation route, and its application does not require harsh conditions, thereby offering a unique balance between high performance and environmental sustainability. This synergy clearly emphasizes the potential of $Fe_3O_4$-BP as a promising adsorbent for practical dye removal applications compared to previously reported materials.

## 3.5 *Proposed adsorption mechanism*

As previously described, the synthesis of $Fe_3O_4$-BP resulted in a noticeable shift of the Fe-O band to around 570 $cm^{-1}$, indicating the interaction between $Fe^{2+}/Fe^{3+}$ ions in the $Fe_3O_4$ lattice and the organic functional groups of BP, suggesting the formation of Fe-O coordination bonds (Fe-OOC-R). The positions and intensities of the -OH (~ 3,425 $cm^{-1}$), C=O (~ 1,620 $cm^{-1}$), and C-O/C-O-C (~ 1,342 and 1,095 $cm^{-1}$) bands were also altered, confirming that the interaction occurred not only physically but also chemically.

Upon adsorption of MV, a shift of the -OH band to 3,377-3,318 $cm^{-1}$ was observed, along with the emergence of a new aromatic band near 1,580 $cm^{-1}$ and increased intensities in the 1,340-1,080 $cm^{-1}$ region. These spectral changes suggest the involvement of hydroxyl, carbonyl, and carboxylate groups in the interaction with MV molecules. The persistence of the Fe-O band at ~ 580 $cm^{-1}$ indicates that the magnetite framework remained stable despite strong interactions with the dye (Figure 7).

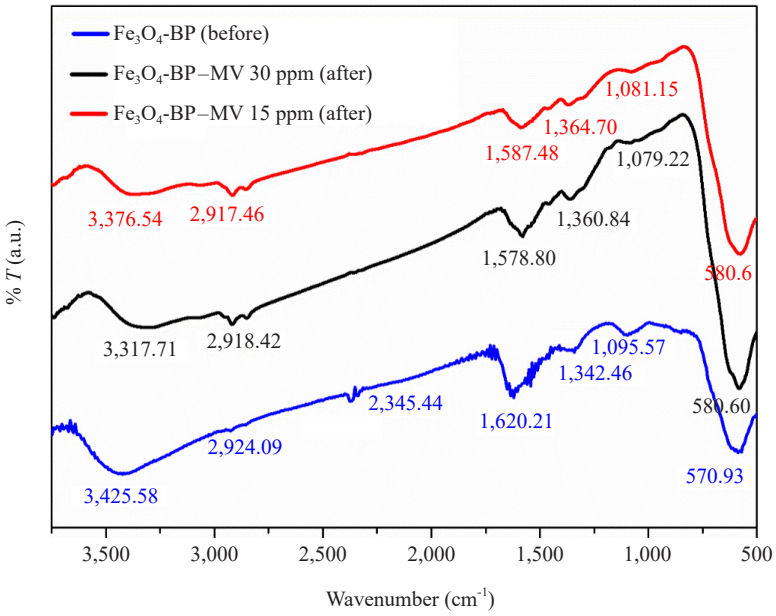


**Figure 7.** FTIR spectra of $Fe_3O_4$-BP adsorbent before adsorption and after methyl violet adsorption

Based on these FTIR changes (-OH shift from ~ 3,425 → 3,377-3,318 $cm^{-1}$, alteration of C=O/C-O bands, the appearance of the aromatic band at ~ 1,580 $cm^{-1}$, and the retention of Fe-O at ~ 570-580 $cm^{-1}$), the adsorption mechanism of MV onto $Fe_3O_4$-BP can be proposed as a combination of: (i) coordination/complexation between carboxylate/carbonyl-OH groups and Fe ions on the surface (inner-sphere complexation), (ii) electrostatic interactions between surface charges and cationic MV, (iii) hydrogen bonding, (iv) $\pi$-$\pi$ interactions between the aromatic rings of MV and the BP organic framework, and (v) pore-filling/intraparticle diffusion.

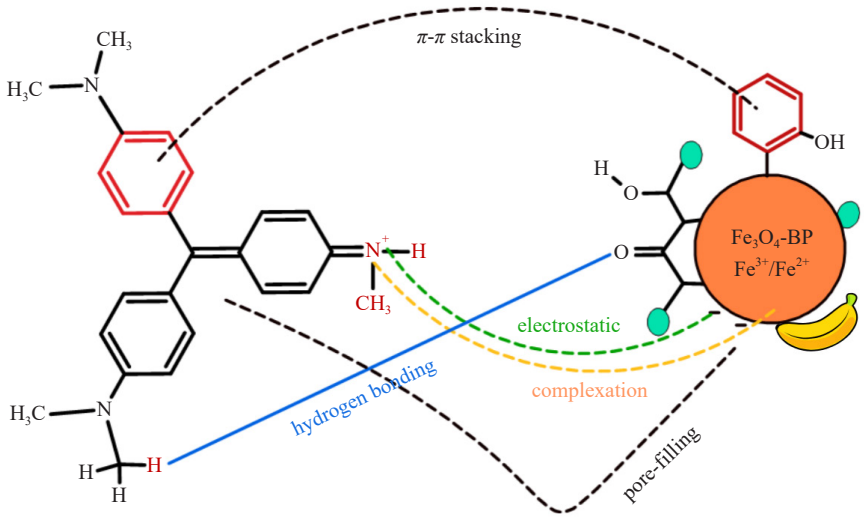


**Figure 8.** Proposed adsorption mechanism of MV on $Fe_3O_4$-BP

The adsorption mechanism of MV onto $Fe_3O_4$-BP is presumed to involve a combination of electrostatic interactions, hydrogen bonding, and $\pi$-$\pi$ stacking between the aromatic rings of polyphenols derived from banana peel biomass and the aromatic structure of MV. The presence of -OH and C=O functional groups on the adsorbent surface further enhances the likelihood of chemical interactions, while the magnetic properties of $Fe_3O_4$ facilitate the easy separation of the adsorbent after adsorption.[35] Since the adsorption isotherm follows the Langmuir model, the adsorption process is dominated by monolayer coverage on homogeneous active sites, while pore-filling effects are considered less significant. In addition, the possibility of complexation between the surface $Fe^{2+}$/$Fe^{3+}$ sites of $Fe_3O_4$ and electron-donating groups from MV molecules (e.g., amine nitrogen) or oxygen-containing groups (-OH, C=O, -COOH) from banana peel extract cannot be excluded, indicating that specific chemisorption may also contribute to the overall adsorption mechanism. The proposed adsorption mechanism is schematically illustrated in Figure 8.

## 4. Conclusion

This study successfully developed an eco-friendly adsorbent material derived from banana peel waste, modified with magnetite ($Fe_3O_4$-BP) through a coprecipitation method. Characterization results confirmed the formation of a crystalline spinel $Fe_3O_4$ structures with the successful integration of functional groups from banana peel extract on the particle surface. The adsorbent exhibited a high adsorption capacity for MV dye, with a maximum capacity of 135 mg/g that fits well with the Langmuir isotherm model, indicating a monolayer adsorption mechanism. MV removal efficiency reached over 95% in simulated real wastewater and could be easily separated using a magnet, with potential for reuse. Thus, the utilization of agricultural waste such as banana peel as a multifunctional material not only enhances the added value of organic waste but also provides a low-cost, eco-friendly, and sustainable solution for textile wastewater treatment.

## Conflict of interest

The authors declare no competing financial interest.

## References


[1] Alsuhybani, M.; Aleid, M.; Alzidan, R.; Bander, K. B.; Alrehaili, A. High removal of methylene blue and methyl violet dyes from aqueous solutions using efficient biomaterial byproduct. *Heliyon* **2024,** *10*(17), e36731.

[2] Syakina, A. N.; Rahmayanti, M. Removal of methyl violet from aqueous solutions by green synthesized magnetite nanoparticles with *Parkia Speciosa Hassk*. peel extracts. *Chem. Data Coll.* **2023,** *44*, 101003.

[3] Bagtache, R.; Trari, M. Synthesis, characterization of $KAlPO_4F$ and its application for methyl violet adsorption. *Appl. Water Sci.* **2024,** *14*(4), 62.

[4] Aguiar, R. A.; Rodrigues, J. S.; De Souza Bernardes, M.; Do Amparo Madureira, J.; Borsagli, F. G. M. The potentiality of reuse industrial waste for diverse water treatment-an overview. *Sustain. Chem. Eng.* **2023,** *4*, 57-69.

[5] Naeem, W.; Haq, F.; Ullah, H.; Khan, A.; Kundi, R.; Bukhari, I.; Farid, A. Sustainable starch strategies: nano and macro adsorbents for the detoxification of synthetic dyes and heavy metals. *Sustain. Chem. Eng*. **2024,** *5*, 426-449.

[6] Faizal, A. N. M.; Wen, C. H.; Putra, N. R.; Zaini, A. S.; Agi, A.; Nordin, A. H.; Zaini, M. A. A. Crayfish shell biochar for methyl violet adsorption: equilibrium and kinetic studies. *Next Sustain*. **2025,** *6*, 100093.

[7] Ngwethe, C. B. N.; Ndongo, G. K.; Tchuifon, D. R. T.; Fotsop, C. G.; Dongmo, D. S. M.; Foko, U. R. N.; Kede, M. C. Regeneration and reusability of bleaching earth as a sustainable material for tartrazine yellow (E102) removal: insights into kinetic mechanisms. *Sustain. Chem. Eng*. **2024,** *5*, 450-470.

[8] Rahmayanti, M.; Syakina, A. N. *Kimia Hijau: Kemajuan Terkini & Prospek Masa Depan [Green Chemistry: Recent Advances & Future Prospects]*; Samudra Biru, 2025.

[9] Prakash, R.; Bharti, R.; Thakur, A.; Verma, M.; Sharma, R. Environmentally benign green approach for the synthesis of IONPs using *Vicia Faba* fruit extract and their antioxidant activities. *Sustain. Chem. Eng*. **2025,** *6*, 11-21.

[10] Al-Khaial, M. Q.; Chan, S. Y.; Abu-Zurayk, R. A.; Alnairat, N. Biosynthesis and characterization of zinc oxide nanoparticles (ZnO-NPs) utilizing banana peel extract. *Inorganics* **2024,** *12*(4), 121.

[11] Utami, M.; Yenn, T. W.; Alam, M. W.; Ravindran, B.; Purnama, I.; Hidayat, H.; Salsabilla, S. N. Efficient photocatalytic bactericidal performance of green-synthesised $TiO_2$/reduced graphene oxide using banana peel extracts. *Heliyon* **2024,** *10*(4), e26636.

[12] Tahar, L. B.; Mogharbel, R.; Hameed, Y.; Noubigh, A.; Abualreish, M. J. A. A. E.; Alanazi, A. H.; Hatshan, M. R. Enhanced removal of the crystal violet dye from aqueous medium using tripolyphosphate–functionalized Zn–substituted magnetite nanoparticles. *Results Chem*. **2025,** *14*, 102152.

[13] Fındık, S. Sono-assisted adsorption of methyl violet 2B using a magnetic kaolin/$TiO_2$/$\gamma$-$Fe_2O_3$ nano composite. *Water Air Soil Pollut*. **2024,** *235*(8), 514.

[14] Molla, W. T.; Kebede, Z.; Tesfaye, M. Innovative salt-free reactive dyeing of cotton using cationization with *Vicia Faba* bean pod waste. *Sustain. Chem. Eng*. **2025,** *6*, 130-145.

[15] Tyagi, P. K.; Gupta, S.; Tyagi, S.; Kumar, M.; Pandiselvam, R.; Daştan, S. D.; Arya, A. Green synthesis of iron nanoparticles from spinach leaf and banana peel aqueous extracts and evaluation of antibacterial potential. *J. Nanomater.* **2021,** *2021*(1), 4871453.

[16] Daffalla, S.; Taha, A.; Da'na, E.; El-Aassar, M. R. Sustainable banana-waste-derived biosorbent for congo red removal from aqueous solutions: kinetics, equilibrium, and breakthrough studies. *Water* **2024,** *16*(10), 1449.

[17] Rahmayanti, M.; Santosa, S. J.; Sutarno, S. Comparative study on the adsorption of $[AuCl_4]^-$ onto salicylic acid and gallic acid modified magnetite particles. *Indones. J. Chem*. **2016,** *16*(3), 329-337.

[18] Kathiresan, K.; Durairaj, S. Green synthesis of iron oxide nanoparticles using date seed extracts for biomedical applications. *Int. J. Environ. Sci. Technol*. **2025,** *22*, 15167-15188.

[19] Piro, N. S.; Hamad, S. M.; Mohammed, A. S.; Barzinjy, A. A. Green synthesis magnetite ($Fe_3O_4$) nanoparticles from Rhus coriaria extract: a characteristic comparison with a conventional chemical method. *IEEE Trans. Nanobiosci.* **2022,** *22*(2), 308-317.

[20] Rauf, A.; Ahmad, Z.; Ajaj, R.; Zhang, H.; Ibrahim, M.; Muhammad, N.; Ullah, I. Green synthesis an eco-friendly route for the synthesis of iron oxide nanoparticles using aqueous extract of *Thevetia peruviana* and their biological activities. *Sci. Rep*. **2025,** *15*(1), 18316.

[21] Bassim, S.; Mageed, A. K.; AbdulRazak, A. A.; Majdi, H. S. Green synthesis of $Fe_3O_4$ nanoparticles and its applications in wastewater treatment. *Inorganics* **2022,** *10*(12), 260.
[22] Siddiqa, A.; Khatun, H.; Mostafa, G. Green synthesis of magnetite: Characterization and comparison with conventional chemical methods. *Modern Chemistry* **2025,** *3*, 53-63.
[23] Elkhateeb, O.; Atta, M. B.; Mahmoud, E. Biosynthesis of iron oxide nanoparticles using plant extracts and evaluation of their antibacterial activity. *AMB Express* **2024,** *14*(1), 92.
[24] Rahmayanti, M.; Syakina, A. N.; Fatimah, I.; Sulistyaningsih, T. Green synthesis of magnetite nanoparticles using peel extract of jengkol (*Archidendron pauciflorum*) for methylene blue adsorption from aqueous media. *Chem. Phys. Lett*. **2022,** *803*, 139834.
[25] Rahmayanti, M.; Syakina, A. N.; Sulistyaningsih, T.; Hastuti, B. Synthesis of magnetite using petai (*Parkia speciosa*) peel extract with ultrasonic waves as reusable catalysts for biodiesel production from waste frying oil. *J. Kim. Sains Apl*. **2023,** *26*(4), 125-132.
[26] Darmawan, M. Y.; Saputra, M. E.; Rumiyanti, L.; Istiqomah, N. I.; Adrianto, N.; Tumbelaka, R. M.; Suharyadi, E. Novel green synthesis approach of $Fe_3O_4$-MSN/Ag nanocomposite using moringa oleifera extract for magnetic hyperthermia applications. *Curr. Appl. Phys*. **2024,** *68*, 242-256.
[27] Rahmayanti, M.; Putra, M. D.; Karmanto; Sedyadi, E. Potential organic magnetic nanoparticles from peel extract of *Archidendron pauciflorum* for the effective removal of cationic and anionic dyes. *Korean J. Chem. Eng*. **2023,** *40*(11), 2759-2770.
[28] Rahmayanti, M.; Yahdiyani, A.; Afifah, I. Q. Eco-friendly synthesis of magnetite based on tea dregs ($Fe_3O_4$-TD) for methylene blue adsorbent from simulation waste. *Communications in Science and Technology* **2022,** *7*(2), 119-126.
[29] Rahmayanti, M.; Santosa, S. J.; Sutarno. Comparative study on the adsorption of $[AuCl_4]^-$ onto salicylic acid- and gallic acid-modified magnetite particles. *Indones. J. Chem.* **2016,** *16*(3), 329-337.
[30] Abdallah, M. A.; Abidli, I.; Lemine, M. A.; Bououdina, M. L. I.; Zougagh, M.; Latrous, L.; Megriche, A. Green pomegranate peel and potato peel starch-derived magnetic nanocomposite as efficient sorbent of ascorbic acid extracted from fruit juices. *Food Bioprocess Technol*. **2025,** *18*(5), 4443-4460.
[31] Ghoohestani, E.; Samari, F.; Homaei, A.; Yosuefinejad, S. A facile strategy for preparation of $Fe_3O_4$ magnetic nanoparticles using *Cordia myxa* leaf extract and investigating its adsorption activity in dye removal. *Sci. Rep.* **2024,** *14*(1), 84.
[32] Ali, N. S.; Jabbar, N. M.; Alardhi, S. M.; Majdi, H. S.; Albayati, T. M. Adsorption of methyl violet dye onto a prepared bio-adsorbent from date seeds: isotherm, kinetics, and thermodynamic studies. *Heliyon* **2022,** *8*(8), e10276.
[33] Keyhanian, F.; Shariati, S.; Faraji, M.; Hesabi, M. Magnetite nanoparticles with surface modification for removal of methyl violet from aqueous solutions. *Arab. J. Chem.* **2016,** *9*, S348-S354.
[34] Bonetto, L. R.; Ferrarini, F.; De Marco, C.; Crespo, J. S.; Guégan, R.; Giovanela, M. Removal of methyl violet 2B dye from aqueous solution using a magnetic composite as an adsorbent. *J. Water Process. Eng*. **2015,** *6*, 11-20.
[35] Sarkar, S.; Tiwari, N.; Behera, M.; Chakrabortty, S.; Jhingran, K.; Sanjay, K.; Tripathy, S. K. Facile synthesis, characterization and application of magnetic $Fe_3O_4$-coir pith composites for the removal of methyl violet from aqueous solution: kinetics, isotherm, thermodynamics and parametric optimization. *J. Indian Chem. Soc*. **2022,** *99*(5), 100447.
[36] Foroutan, R.; Mohammadi, R.; Ahmadi, A.; Bikhabar, G.; Babaei, F.; Ramavandi, B. Impact of ZnO and $Fe_3O_4$ magnetic nanoscale on the methyl violet 2B removal efficiency of the activated carbon oak wood. *Chemosphere* **2022,** *286*, 131632.